Field Evaluation of Low-cost Electrochemical Air Quality Gas Sensors at Extreme Temperature and Relative Humidity Conditions

Roubina Papaconstantinou[1], Marios Demosthenous[1], Spyros Bezantakos[1], Neoclis Hadjigeorgiou[1], Marinos Costi[1], Melina Stylianou[2], Elli Symeou[2], Chrysanthos Savvides[3], George Biskos[1,4]

[1]Climate and Atmosphere Research Centre, The Cyprus Institute, Nicosia 2121, Cyprus
[2]Medisell Co Ltd, Nicosia 2033, Cyprus
[3]Ministry Labour Welfare and Social Insurance, Department of Labour Inspection, Nicosia 1463, Cyprus
[4]Faculty of Civil Engineering and Geosciences, Delft University of Technology, Delft 2628CN, The Netherlands

Correspondence to: George Biskos (g.biskos@cyi.ac.cy; g.biskos@tudelft.nl)

Abstract. Modern electrochemical gas sensors hold great potential for improving practices in Air Quality (AQ) monitoring as their low cost, ease of operation and compact design can enable dense observational networks and mobile measurements. Despite that, however, numerous studies have shown that the performance of these sensors depends on a number of factors (e.g., environmental conditions, sensor quality, maintenance and calibration, etc.), thereby adding significant uncertainties in the reported measurements and large discrepancies from those recorded by reference-grade instruments. In this work we investigate the performance of electrochemical sensors, provided by two manufacturers (namely Alphasense and Winsen), for measuring the concentrations of CO, NO_2, O_3 and SO_2. To achieve that we carried out collocated yearlong measurements with reference-grade instruments at a traffic AQ monitoring station in Nicosia, Cyprus, where temperatures ranged from ca. 0 °C in the winter, to almost 45 °C in the summer. The CO sensors exhibit the best performance among all the ones we tested, having minimal mean relative error (MRE) compared to reference instruments (ca. -5%), although a significant difference in their response was observed before and after the summer period. At the other end of the spectrum, the SO_2 sensors reported concentration values that were at least one order of magnitude higher than the respective reference measurements (with MREs being more than 1000% for Alphasense and almost 400% for Winsen throughout the entire measurement period), which can be justified by the fact that the concentrations of SO_2 at our measuring site were below their limit of detection. In general, variabilities in the environmental conditions (i.e., temperature and relative humidity) appear to affect significantly the performance of the sensors. When compared with reference instruments, the CO and NO_2 electrochemical sensors provide measurements that exhibit increasing errors and decreasing correlations as temperature increases (from below 10 to above 30 °C) and RH decreases (from > 75 to below 30%). Interestingly, the performance of the sensors was affected irreversibly during the hot summer period, exhibiting different response before and after that, and resulting to a signal deterioration that was more than twice as that reported by the manufacturers. With the exception of the Alphasense NO_2 sensor, all LCSs exhibited measurement uncertainties that were much higher, even at the beginning of our measurement period, compared to those required for qualifying the sensors for indicative air quality measurements according to the respective EC Directive. Overall, our results show that the response of all LCSs is strongly affected by the environmental conditions, warranting further investigations on how they are manufactured, calibrated and employed in the field.

1 Introduction

35   Air pollution accounts for more than 7 million premature deaths around the globe on an annual basis (Lelieveld et al., 2020), making it the fourth greatest overall risk factor for human health (Juginovic et al., 2021). Recognising this risk, the concentration of key pollutants has to be continuously monitored, especially in the urban environment, in order to ensure that those do not exceed certain limit values. Although wide networks of Air Quality (AQ) monitoring stations have been established in many cities around the globe for this reason, the spatial distribution of the observations is still limited for

40   providing detailed AQ mapping over urban agglomerates. This, in turn, limits our ability to effectively associate urban air pollution with potential human health effects, and to design effective mitigation strategies.

    Building AQ monitoring networks that go far beyond the current state of art with respect to their spatial coverage is limited by the required high capital, operational and maintenance costs. The city of Paris, for instance, operates 13 measuring sites (AIRPARIF, 2018), whereas in London, AQ is monitored at around 100 locations (Greater London Authority, 2018). Although

45   these numbers are seemingly high, they correspond to a spatial coverage of the order of one station over a few tens of square kilometres. This limitation can be lifted by employing Low-Cost Sensors (LCSs) in dense observational networks that can enable quick and effective identification of pollution sources and determination of concentration gradients over specific areas.

    According to the World Meteorological Organization (WMO), LCSs are defined as systems that are at least one order of magnitude less expensive compared to reference instruments (WMO, 2018). Electrochemical (EC) sensors, which fall into this

50   category, have received great attention in recent years as their low cost, compact size and response time (in the order of a minute) can enable their use in dense AQ monitoring networks and easy-to-carry-out mobile measurements. The low price of these sensors, however, comes at a cost in performance and in the quality of the data they provide compared to reference grade instruments, which can be attributed to a number of factors including cross-sensitivities (Lewis et al., 2015; Mead et al., 2013), signal drifts over time and low life expectancies (Mead et al., 2013; Smith et al., 2017; Popoola et al., 2016; Hagan et al.,

55   2018), low sensitivities (Borrego et al., 2016), and variabilities related to environmental conditions (Mead et al., 2017; Jerrett et al., 2017; Spinelle et al., 2015; Spinelle et al., 2017; Cross et al., 2017; Pang et al., 2017; Aleixandre et al., 2012; Masson et al., 2015).

    An increasing number of studies has investigated the performance of LCSs under different conditions (Hagan et al., 2018; Mead et al., 2013; Jerrett et al., 2017; Cross et al., 2017; Jiao et al., 2016; Bílek et al., 2021; Collier-Oxandale 2020). Closer

60   comparison of the results from some of the above-mentioned studies, in which the performance of the same sensors (i.e., Alphasense B series) was tested but at different locations and conditions, shows that the variability of the environmental conditions plays a significant role, provided the concentrations of the target gases are above their limit of detection (LoD) (Borrego et al., 2016; Mead et al., 2017; Cross et al., 2017; Bauerová et al., 2020; Karagulian et al., 2019). In a study carried out in Norway, during which the temperature and relative humidity (RH) varied from −0.7 to 23.3 °C and from 19 to 98%,

65   respectively, the mean bias error (MBE) of the measurements reported by the CO and NO_2 LCSs when compared with reference measurements were respectively −147.2 and 13.3 ppb, whereas the associated correlations (R^2) were 0.36 for the CO

and 0.24 for the NO₂ LCS (Mead et al., 2017). In a similar study carried out in Portugal, where the temperature varied from 15 to 30 °C and RH from 39 to 87%, the overall performance of the same sensors was better, exhibiting lower averaged MBEs (-0.025 ppb for CO and 7.1 ppb for NO_2) and higher R^2 (0.76 for CO and 0.58 for NO_2; Borrego et al., 2016).

70   Operating temperature and RH are two of the most important factors affecting the performance of EC sensors mainly because they employ aqueous electrolytes containing sulphuric acid for the transfer of charges between the measuring and the reference electrodes. The concentration of sulphuric acid in the electrolyte is 5 M, which requires 60% RH at 20 °C in ambient air to be in equilibrium (Alphasense Application Note AAN106, 2013). Exposure of the sensors to RH levels less than 60% can in principle lead to evaporation of the solvent (i.e., water), whereas the opposite can happen at RH conditions above 60%.

75   According to the manufacturer, the Alphasense EC sensors can provide meaningful measurements even when exposed to RH values down to 15% or up to 90% at ambient temperature as long as they have enough time to equilibrate to the new conditions; i.e., several days. Ideally, when EC sensors are exposed over long periods to RH values far from 60%, they need to be recalibrated at the new RH conditions. However, considering that ambient RH is highly variable, and that it can change significantly within a few hours, using RH-dependent calibration turns out to be impractical.

80   It should be noted that field tests of LCSs reported in the literature were conducted at different locations, seasons, and durations that range from 2 weeks (Borrego et al., 2016) to 4.5 months (Cross et al., 2017). This makes any direct comparison and further analysis of the data for understanding how the environmental conditions affect the performance of the LCSs highly challenging (Karagulian et al., 2019). In addition to the potential effects of the environmental conditions on the accuracy of LCSs, the long-term performance of LCSs can systematically vary over time as they can exhibit significant signal drifts (WMO, 85   2018; Jiao et al., 2016; Masson et al., 2015). To address these issues, we urgently need systematic observations at different locations and conditions over long periods of time.

     In this work we compare yearlong measurements of the concentration of key gaseous pollutants (i.e., CO, NO₂, O₃ and SO₂) reported by low-cost EC sensors, manufactured by Alphasense and Winsen, and by reference-grade instruments. The measurements took place at a traffic station in the city of Nicosia, Cyprus, where the LCSs were exposed to highly variable 90   gaseous concentrations (which were affected both by local and regional pollution sources), and variable environmental conditions. The site is characterised by a high number of sunny days and long hot summers when the temperature and RH can reach values up to ca. 50 °C and below 10%, respectively, providing a unique setting for testing the performance of these sensors under extreme conditions.

2 Methods

95   ### 2.1 Low-cost gas sensors

EC sensors manufactured by Alphasense and Winsen EC were tested in this study. More specifically, we employed the analogue Alphasense B-series gas sensors (Models CO-B41, NO₂-B43F, OX-B431, and SO₂-B4) and the digital Winsen ZE12 model sensors configured by the manufacturer to measure the concentration of CO, NO₂, O₃ and SO₂.

The operating principle of EC sensors relies on redox reactions that take place on the surface of their sensing electrode, which is also referred to as the working electrode (WE). More specifically, the gas molecules reaching the surface of the WE get either oxidised or reduced, consequently providing or capturing electrons to/from the system depending on their electronegativity. An EC cell is completed by the so-called counter electrode (CE) that balances the charge variabilities from the reactions at the surface of the WE. This charge balancing happens by transferring electrons through an electrolyte serving as the medium for transporting the charge carriers from one electrode to the other. The electrical signal (i.e., current) produced by this process is proportional to the concentration of the reducing/oxidising gas interacting with the WE. In some EC sensors, a reference electrode (RE) is used to maintain the potential of the WE at a fixed value.

All EC LCSs employed in this work use the above-mentioned three-electrode configuration. The Alphasense sensors employ an additional electrode, namely the auxiliary electrode (AE), which has similar characteristics to those of the WE, but is incorporated in the cell in a way that it is not exposed to the target gas. A background current, caused by all other factors except the interaction of the WE with the target gas, is induced on the AE. It should be noted that the WE measures the combined current, which is the sum of the background current and the current induced by the target gas when reacting with it. The AE current is then subtracted from the WE current, giving the compensated WE current (i.e., without the background signal) that corresponds solely to the interaction of the sensing electrode with the target gas.

The specifications of all the LCSs we employed are provided in Tables S1 in the supplement. For our tests the sensors were placed in two waterproof boxes – one containing the Alphasense and the other the Winsen LCSs (cf. Fig. 1a and 1b, respectively) – with the sensing side facing outside as shown in Fig. 1c. The boxes, referred to as the AQ monitors from this point onwards, were protected with a reflective cover to avoid direct exposure to sunlight, and attached on a railing within one-meter distance from the inlet of the reference instruments (cf. Fig. 1d). Both monitors were installed at the rooftop of the reference AQ monitoring station (see description further below) from October 2019 to December 2020, and operated continuously, with some interruptions during the high temperatures season.

To run the AQ monitors and record the data from the LCSs we built an electronics circuit board (cf. Figures 1a and 1b) comprised of a microcontroller (Atmel, Model AVR Mega 2560), a Real Time Clock (RTC; Maxim, Model DS3231), a display and a Secure Digital (SD) card. For the Alphasense gas sensors that have a dual analogue output, an Analog to Digital Converter (ADC; Texas Instruments, Model ADS1115) was employed to convert their analogue voltage signals to digital values. The Winsen LCSs have a digital output in Universal Asynchronous Receiver-Transmitter (UART) protocol, so no conversion was needed. The data from the LCSs were stored on the SD cards every 2 seconds for the Alphasense sensors and every 5 seconds for the Winsen sensors. The RTC, ADC and the display communicated with the microcontroller via an Inter-Integrated Circuit (I2C), whereas the SD card was accessed via Serial Peripheral Interface (SPI) protocol. Figure S1 in the supplement shows the schematic of the electronic circuit employed in the AQ monitors.

2.2 Measurement site

The site used for our measurements is a traffic AQ monitoring station in Nicosia, Cyprus, with latitude and longitude coordinates 35°9'7.20"N, 33°20'52.03"E. The station is located at a distance of ten metres from one of the main and busiest city avenues (cf. Fig. 2), which is typically congested during the morning and the afternoon rush hours. The site is considered a reference AQ station as the measurements follow the relevant European Commission (EC) Directives and the corresponding national laws defining the specifications that the employed instruments must meet, as well as the measurement procedures that must be followed, which are also in accordance with international quality standards (Directive 2008/50/EC, 2008). The reference instruments used at the station together with their characteristics are listed in Table S2 of the supplement.

We should highlight here that Cyprus is an island in the Eastern Mediterranean; a region that is a crossroad of polluted air masses coming from three continents (namely Europe, Asia and Africa; Lelieveld et al., 2002). Local sources contribute to the background AQ of the region, creating a highly interesting blend of air pollutants. In addition, the region is characterised by a high number of sunny days with intense ultraviolet (UV) radiation, resulting to a strong atmospheric photochemical activity compared to other European countries (Vrekoussis et al., 2022). According to the national authority for regulatory monitoring, the main sources of CO observed on the island are related to local fossil fuel burning (i.e., energy production, transportation and central heating) having typical annual concentrations of more than 250 µg/m^3 (153 ppb; DLI Annual Technical Report Air Quality, 2020). The primary sources of NO_2 and SO_2 emissions are also from fossil fuel burning, having typical mean annual concentrations of more than 15 µg/m^3 (ca. 9 ppb) and 2 µg/m^3 (ca. 1 ppb), respectively (DLI Annual Technical Report Air Quality, 2020), whereas the annual mean concentrations of O_3 is ca. 70 µg/m^3 (ca. 35 ppb).

2.3 Calibration of the LCSs

The Alphasense gas sensors employed in this work were accompanied by an Individual Sensor Board (ISB), which converts the signal from the WE and AE to voltages and facilitates data acquisition using ADCs. The electronic and zero offsets of the WE and AE signals, as well as the sensitivity and temperature correction factors were also provided by the manufacturer for each sensor following laboratory calibration. These values were used to convert the measured signals to concentrations of pollutants by first calculating the corrected WE voltage value and then dividing by the sensor sensitivity. The manufacturer provides four different equations for the conversion of the raw signals from the WE and the AE to gas concentrations (expressed in ppb) for each sensor. The equations used in this work were the ones converting the raw signals to concentrations that are in better agreement with those reported by the reference instruments. For the CO and O_3 sensors this is:

$$C = \frac{V_{WEc}}{S} = \frac{(V_{WEu} - V_{WEe}) - n_T * (V_{AEu} - V_{AEe})}{S}, \tag{1}$$

where V_{WEu} is the uncorrected raw WE output, V_{WEe} is the WE electronic offset on the ISB, n_T is a temperature dependent correction factor, V_{AEu} is the uncorrected raw AE output, V_{AEe} is the AE electronic offset on the ISB, and S is the sensitivity. We should note here that all the electrode signals are provided in mV, whereas the sensitivity of the sensors is expressed in mV/ppb. To account for cross-sensitivity of the O_3 LCS from NO_2, the first term in the nominator of Eq. 1 becomes V_{WEu} −

$V_{WEe} - V_{WEc(NO2)}$, where $V_{WEc(NO2)}$ is the voltage induced on the working electrode, calculated using the NO_2 concentration measured from the NO_2 LCS, multiplied by the sensitivity (expressed in mV/ppb) of the O_3 sensor on NO_2, following the guidelines by the manufacturer (Alphasense Application Note AAN 803-05, 2019). For the NO_2 and the SO_2 sensors, the equation yielding concentration values that compared better with those of the reference instrument is:

$$C = \frac{V_{WEc}}{S} = \frac{(V_{WEu} - V_{WEe}) - k_{T*}\left(\frac{V_{WEo}}{V_{AEo}}\right)(V_{AEu} - V_{AEe})}{S}.$$ (2)

Here V_{WEo} is the WE output in zero air (i.e., air without the target gas), V_{AEo} is the AE output in zero air, and k_T is the temperature dependent correction factor.

Temperature is used as input for the calculation of the correction factors n_T and k_T in Eq. (1) and (2). The values of n_T and k_T are provided by the manufacturer for specific temperatures, ranging from ca. -30 to 50 °C with 10 °C interval, are shown in the supplement (Table S3). It should be noted that for a more accurate calculation of the temperature correction factors in our analysis, we used linear (for CO) or spline (for NO_2, O_3 and SO_2) interpolations, as shown in Figure S2 in the supplement. While a temperature/RH sensor was included inside the two AQ monitors, the temperatures used as input for the calculation of the correction factors n_T and k_T are the ones measured by the reference thermometers at the station. We should note here that the temperature and RH sensor used in the two AQ monitors, recorded measurements that deviated substantially from those reported by the reference sensors, and thus were not used for determining the concentrations from the LCSs.

The Winsen ZE12 gas sensors are general-purpose sensors that can measure the concentration of CO, SO_2, NO_2 and O_3 based on the EC sensor principle. In contrast to their Alphasense counterparts, these sensors do not come with a specific calibration equation to account for temperature variabilities. Instead, measurements from a built-in temperature sensor are used internally to capture respective variabilities, providing signal outputs that are directly expressed as concentrations (ppb). It should be noted that an offset of ca. 400 ppb in the raw measurements from the Winsen CO LCS was observed throughout the entire period of our study, and that this value has been subtracted from the reported data to facilitate comparison with the measurements by the respective reference instrument.

2.4 Data Analysis

As stated above, the WE and AE outputs from the Alphasense LCSs were recorded every 2 seconds whereas the concentrations from the Winsen LCSs were recorded every 5 seconds. All LCS measurements were averaged over a period of an hour for direct comparison with the observations provided by the reference instruments. After converting raw signals to concentrations, negative values were omitted. The effect of the environmental parameters (i.e. temperature and RH) on the performance of the sensors was assessed by dividing the whole dataset into different temperature (i.e., < 10, 10-20, 20-30, and > 30 °C) and RH (i.e., < 30, 30-55, 55-75, and > 75%) ranges. These ranges were selected considering the minimum and maximum temperature and RH values encountered during our measurement period and the conditions that the LCSs are calibrated in the laboratory by the manufacturer (i.e., T = 20 °C and RH = 60%).

The performance of the LCSs is evaluated by directly correlating and comparing the reported concentrations with measurements by the respective reference instruments to determine the associated errors. The parameters used to do so were
the coefficient of determination (R^2), the mean bias error (MBE), the mean relative error (MRE), the mean absolute error (MAE), and the normalised root mean square error (NRMSE), defined respectively as follows:

$$R^2 = 1 - \frac{\sum_{i=1}^{N}(C_{LCS,i} - C_{ref,i})^2}{\sum_{i=1}^{N}(C_{LCS,i} - \overline{C_{ref}})^2} \tag{3}$$

$$MRE = \frac{1}{N}\sum_{i=1}^{N}\left(\frac{(C_{LCS,i} - C_{ref,i})}{C_{ref,i}}\right) \times 100 \tag{4}$$

$$MBE = \frac{1}{N}\sum_{i=1}^{N} C_{LCS,i} - C_{ref,i} \tag{5}$$

$$MAE = \frac{1}{N}\sum_{i=1}^{N}\left|C_{LCS,i} - C_{ref,i}\right| \tag{6}$$

$$NRMSE = \frac{1}{\overline{C_{LCS}}}\sqrt{\frac{\sum_{i=1}^{N}(C_{LCS,i} - C_{ref,i})^2}{N}} \tag{7}$$

In all these equations, N is the total number of data points (i.e., time-tagged pairs of measurements from the LCSs and the reference instruments), whereas $C_{LCS,i}$ and $C_{ref,i}$ are the concentrations (expressed in ppb) measured respectively by the LCSs and the reference instruments at time *i*. To evaluate the degradation of sensors over time, we used the normalised MRE that is defined as follows:

$$NMRE = \frac{MRE_{end} - MRE_{bgn}}{MRE_{bgn}}. \tag{8}$$

Here MRE_{bgn} and MRE_{end} correspond to the MRE at the beginning and at the end of the measurement period, respectively.

In addition to assessing the performance of the sensors in terms of how well they correlate and agree with reference instruments, we determined whether the data they provide meet internationally accepted quality objectives. According to the 2008/50/EC AQ Directive (EC, 2008), the relative expanded uncertainty (REU) of the measurements can be used to assess the degree to which certain data quality objectives are met for specific LCSs. REU is determined at fixed concentrations, which are typically the limit values set by directives and/or authorities, and are determined by collocating the LCSs with reference grade instruments at AQ monitoring stations. In general, the REU is defined as:

$$REU = \frac{2\sqrt{\frac{RSS}{N-2} + (\lambda - (\theta_1 - 1)^2) \times U_{ref}^2 + (\theta_0 + (\theta_1 - 1) \times C_{ref,i})^2}}{C_{ref,i}} \times 100\%. \tag{9}$$

Here N is the number of data pairs, λ is the ratio of the variances of the LCSs over those of reference measurements which is typically assumed to be unity (Walker et al., 2020), θ_0 and θ_1 are estimated coefficients obtained via orthogonal regression between reference and LCS measurements (cf. Table S7 in the supplement), and U_{ref} is the standard uncertainty of the reference measurements. RSS in Eq. (9) is the sum of the squared residuals determined by:

$$RSS = \sum_{i=1}^{N}(C_{LCS,i} - \theta_0 - \theta_1 \times C_{ref,i})^2. \tag{10}$$

220 A LCS can be used for indicative measurements if the REU determined at the limit value (or target value in the case of O_3) remains within 25% for CO, NO_2 and SO_2, or 30% for O_3 (Directive 2008/50/EC).

3 Results and Discussion

3.1. Statistics

Figure 3 provides a 2-month (over December 2019 and January 2020) snapshot of the hourly-averaged concentration
225 measurements by the LCSs and the reference instruments. The CO and NO_2 sensors from both manufacturers are capable of qualitatively reproducing the reference measurements (cf. Figures 3a and 3b, respectively). In contrast to the case of CO and NO_2, the SO_2 and O_3 concentrations measured by the LCSs exhibit a difference of two to three orders of magnitude compared to the reference measurements. For display purposes, the SO_2 LCS measurements shown in Fig. 3 were divided by 10; the results discussed in the rest of the paper, however, correspond to the real recorded values.

230 Aggregated statistics from all the measurements and for each sensor during the entire testing period are provided in Table 1. Overall, the CO measurements by the LCSs from both manufacturers show better agreement with those reported by the respective reference instruments (cf. mean values in Table 1) compared to the rest sensors tested. Both CO sensors capture the temporal concentration variability attributed primarily to the morning and afternoon traffic pollution. The Alphasense CO LCS exhibits the lowest MRE, with a value of -4.7%, and the highest correlation ($R^2 = 0.54$) compared to the respective Winsen
235 LCS (MRE = 35.1%, $R^2 = 0.25$).

The measurements recorded by the NO_2 LCSs from both manufacturers followed similar temporal patterns to those of the reference instrument, exhibiting moderate, but similar, correlations (i.e., $R^2 = 0.10$ for Alphasense and $R^2 = 0.29$ for Winsen). Overall, both LCSs overestimated the NO_2 concentrations, with the Alphasense NO_2 sensor exhibiting better performance compared to that of Winsen as indicated by the MRE (53.7% against 104.8%, respectively) and MAE (10.8 against 15.1 ppb,
240 respectively) shown in Table 1. The higher errors associated with the NO_2 LCSs of both manufacturers can be attributed to cross sensitivities with other gaseous pollutants.

The Alphasense O_3 sensor overestimated significantly the absolute reference concentrations, exhibiting high MRE (923.1%) and MAE (48.1 ppb) values. On the other hand, the Winsen O_3 sensor mainly underestimated the actual concentration, exhibiting a significantly lower MRE (44.0%) and MAE (16.5 ppb) compared to its Alphasense counterpart.
245 The reported correlation coefficients of both O_3 sensors with the reference instruments were among the lowest of all the LCSs tested (R^2 was 0.05 for the Alphasense and 0.06 for the Winsen O_3 sensor).

The performance of the SO_2 sensors was the poorest compared to those of the rest of the LCSs mainly because the concentrations at the monitoring station, as those were reported by the reference instruments, were quite low (ranging between 2 and 4 ppb during the study period) and always below the LoD of the LCSs: i.e., 5 ppb for the Alphasense and 15 ppb for the
250 Winsen sensor.

Figure 4 shows the correlation of the measurements recorded by the Alphasense (Fig. 4a-d) and by the Winsen (Fig. 4e-h) LCSs with those provided by the respective reference instruments. The associated errors between the LCS and reference instrument measurements are provided in the supplement (cf. Fig. S3). The performance of LCSs appears to degrade from left to right in Fig. 4, with the CO and NO_2 exhibiting the best performance, whereas O_3 and SO_2 the worst.

255   Two distinct linear data clusters are observed for the Alphasense CO sensor (cf. Fig. 4a), which can be attributed to the degradation of the sensor performance from its exposure to the high temperatures and low RH values during the summer period. This is more clearly shown in Fig. S4a in the supplement, which depicts the same data tagged by the time that the measurements were recorded. We should note here that the temperatures and RH conditions that the LCSs were exposed to during the entire measuring campaign ranged respectively from -0.4 to 42.4 °C and from 2.8 to 96.8%. More specifically, the

260   temperature ranged from 14.1 to 42.4 °C during summer (Jun.-Aug. 2020) and from -0.4 to 21.3 °C during winter (Dec. 2019-Feb. 2020), while the RH varied from 2.81 to 95.19%, and from 32.7 to 96.81%, during summer and winter, respectively. As discussed in Section 1, exposing the EC LCSs to extreme temperature and RH conditions can cause irreversible changes of their electrolyte solution, leading to a behaviour that is noticeably different before and after that. The phenomenon is also observed for the Winsen CO LCS (cf. Fig. S4b in the supplement), but to a less extent mainly due to the limited data acquired

265   after summer with that sensor. The same is not evident for the rest of the sensors. However, we should note here that correlation with reference instruments was not as strong in those cases, potentially due to the small extent of data clustering before and after the summer period, and to the fact that the amount of measurements used for the analysis was less than that of the CO Alphasense LCS (cf. Table 1).

     The data provided in Table 1 and Fig. 4 indicate that the O_3 and SO_2 LCSs by both manufacturers exhibit extremely high

270   MREs and/or low correlations against the respective reference instruments. The high errors of the Alphasense O_3 measurement can be associated to interferences with NO_2. This is in fact taken into account, as the signal from the NO_2 LCS (mV) is subtracted from the O_3 sensor signal following the guidelines by the manufacturer (cf. first term in the nominator of Eq. (1)). Although this correction is used for the performance analysis of the Alphasense O_3 LCS, it yields a measurement error that is higher compared to the case when the correction is not applied (cf. Fig. S6), most likely due to error propagation from the

275   signal of the NO_2 sensors to the reported concentrations of O_3. We should note that no cross-sensitivity correction is provided by Alphasense for the case of the NO_2 sensor. It is well possible that the Winsen NO_2 and O_3 LCSs are also prone to cross-sensitivities, despite the fact that the manufacturer does not provide any information or a correction for that. Investigating that, however, is beyond the scope of this study, and thus the respective measurements were used as provided by the sensors. For the case of the SO_2 LCSs, as indicated above, most of the measurements fall below the threshold of their LoD (cf. Table S1).

280   Considering the above, the performance of the O_3 and SO_2 LCSs was not assessed further, and thus we will not discuss the respective measurements from this point onwards.

3.2. Effect of temperature

Figures 5 and 6 show the correlation between the CO or the NO_2 measurements recorded by the Alphasense (Figures 5a-d and 6a-d) and the Winsen (Figures 5e-h and 6e-h) LCSs, with the respective measurements provided by the reference instruments at four temperature ranges: T < 10 °C, 10-20 °C, 20-30 °C and > 30 °C. Statistics and parameters of linear regression fittings to the data at each temperature range are provided in Table 2.

Overall, the trend is characterised by a decreasing correlation between LCS and reference measurements as the temperature increases. More specifically, the Alphasense CO sensor (cf. Fig. 5a-5d) correlates well with the reference instrument at temperatures below 20 °C, than at higher temperatures (e.g., R^2 is 0.70 for T 10-20 °C and 0.05 for T > 30 °C; cf. Table 2). Similarly, the Winsen CO sensor (cf. Fig. 5e-5h) exhibits strong correlation with reference measurements at temperatures below 10 °C (e.g., $R^2 = 0.62$; cf. Table 2), but deteriorates at higher temperatures, exhibiting anti-correlation above 20 °C (cf. Table 2).

The NO_2 sensors exhibit the highest correlation with reference measurements at temperatures below 10 °C, and the lowest above 30 °C. More specifically, the Alphasense NO_2 sensor (cf. Fig. 6a-d) exhibits high correlations with the reference instrument ($R^2 = 0.80$) below 10 °C, which is similar to that of the Winsen NO_2 sensor (cf. Fig. 6e-h; $R^2 = 0.59$). Above this temperature, the sensor performance deteriorates at the extent that it becomes incapable of capturing the variability of the NO_2 concentrations (cf. Fig. 6f-6h). In addition to that, NO_2 LCSs can have (according to Alphasense) interferences from O_3 (Li et al., 2021), which is typically found in high concentrations during high UV radiation periods of the summer months in Cyprus (Vrekoussis et al., 2022), but this is not accounted for by the manufacturer as discussed also in the previous section.

The extreme temperatures that the LCSs have been exposed to over the summer period, have significantly affected their performance during the two cold periods of our tests. This is more pronounced for the CO sensors as reflected by the two distinct data clusters in Fig. 5a and 5e, as well as in Fig. S4 in the supplement. As discussed above, this can be attributed to changes of electrolyte water content during high temperature seasons as in the case of the Alphasense CO LCS (cf. Section 3.1). It should be noted that even though the sensors were not operating during the summer months, they were exposed to ambient temperatures (up to 45 °C), while their main body containing the electrolyte was at even higher values (i.e., > 50 °C) during midday, as a result of heat built up within the cases of the AQ monitors.

3.3. Effect of relative humidity

Figures 7 and 8 show respectively the correlation between CO and NO_2 measurements recorded by the Alphasense and the Winsen LCSs, and those provided by the respective reference instruments at four RH ranges: < 30%, 30-55%, 55-75% and > 75%. Statistics and parameters of linear regression fittings at each RH range are provided in Table 3.

The correlation between the LCSs and the reference instruments increases with increasing RH. The Alphasense CO sensor (cf. Fig. 7a-7d) correlates better with the reference measurements at RH values above 75% (i.e., R^2 up to 0.70; cf. Table 3), than at drier conditions (i.e., $R^2 = 0.20$ for RH < 30%; cf. Table 3). In a similar manner, the Winsen CO sensor (cf. Fig. 7e-7h)

exhibits strong correlation with reference measurements at RH values above 75% (i.e., $R^2 = 0.57$; cf. Table 3), but deteriorates at lower RH values.

The NO$_2$ LCSs from the two manufacturers exhibit the highest correlation with reference measurements at RH > 75%, but decrease substantially at lower RH values. More specifically, the Alphasense NO$_2$ sensor (cf. Fig. 8a-d) exhibits higher correlations with the reference instrument ($R^2 = 0.56$) at RH > 75%, compared to lower RH levels (i.e., $R^2 = 0.30$ at RH < 30%). The measurements by the Winsen NO$_2$ LCS (cf. Fig. 8e-h) exhibited similar correlations with its Alphasense counterpart at RH > 75%, but its performance deteriorates at RH values below 75%, until it becomes incapable of capturing the variability of the NO$_2$ concentrations (cf. Fig. 8e-6g). Since low RH is associated with elevated temperatures, and vice versa (cf. Fig. S5 in the supplement), it appears that the degraded performance noted at high temperatures for the CO and NO$_2$ sensors from both manufacturers corresponds to that observed at the low RH conditions (cf. correlations provided in Fig. 5d, 5h, and 6d, 6h in correspondence with those in Fig. 7a, 7e and 8a, 8e).

The Alphasense EC gas sensors are calibrated in the lab at a fixed RH of 60%, but according to the manufacturer they can operate in the RH range of ca. 15 to 90%. Long exposures of the sensors to an environment with a RH below or above 60% can affect their performance due to evaporation or condensation, respectively, of water from/to the electrolyte (Alphasense Application Note AAN106, 2013). In principle, re-calibration of these sensors would be appropriate, provided that they equilibrate to the new RH conditions. In reality however, this is not so practical to do in the field because the period required for the sensor to reach equilibrium is much longer (ranging from a few days to almost a month) compared to the daily variability of ambient RH.

As discussed in Section 3.2, even though the sensors were not operating during the summer months, their main body, which was in the AQ monitors, was exposed to extreme conditions (temperatures > 50 °C and RH < 10%). In addition to that, the sensors were exposed to high diurnal temperature and RH variabilities, ranging from 20 °C during the night to 40 °C during the day, with respective values of RH ranging from 20 to 80% (cf. Fig. S5 in the supplement), and thus they never had enough time to equilibrate to any RH. These conditions had an impact on the performance of the sensors which was not only temporary (i.e., during the summer period), but persisted even after summer as discussed above (cf. Section 3.1).

3.4. Degradation of Low Cost EC Sensors

Figures 9 and 10 show how the measurements from the CO and NO$_2$ LCSs respectively compare with those from reference instruments over 6 consecutive days at the beginning and at the end of the measurement period. Table 4 summarises the results providing the median MBE, MRE, and NMRE, along with the temperature, RH and reference concentration corresponding to the two periods.

Evidently, all LCSs exhibit degradation of their performance over time, expressed as an increase of the median MBE, in terms of absolute values, after the end of our measurement period that lasted for one year (cf. Fig. 9-10). Similarly, an increase of the MRE values, again in absolute terms, is also observed. For the Alphasense CO the MRE changes from almost 32 to less than -52% from the start to the end of the field campaign, yielding an NMRE of -2.6, whereas for the Alphasense NO$_2$ sensors

the MRE changes from almost 8 to around 23%, with a NMRE of 1.9. These results are in line with those reported by Li et al. (2021), who showed that most of the Alphasense NO_2 sensors they tested exhibited significant deterioration of their performance after long-term (200 to 400 days) deployment. The Winsen LCSs exhibited similar degradation in performance, with NMRE values of 2.0 for the CO and 1.3 for the NO_2 sensors. We should note here that to make a fair comparison of the performance of each sensor at the beginning and the end of the measurement campaign, we made an effort to select measurements corresponding to similar temperature and RH conditions during the two periods. This was feasible for the datasets of the Alphasense sensors but not so easy for the Winsen, as those were not always functional after the summer period, yielding significantly less measurements during that period as indicated in Table 1 and reflected by the high temperature differences in the two periods analysed here (cf. Table 4).

According to specifications provided by the manufacturers, the lifespan of EC LCSs ranges from 2 to 3 years, and specifically for the Alphasense sensors the signal deterioration should be within less than 50% over a period of 24 months (cf. Table S1 in the supplement and references therein). Assessing that based on field measurements however, is not so straightforward due to simultaneous variabilities in both the concentration of the target gases and the meteorological conditions over time. To overcome this problem, we selected two 2-month periods, one at the beginning (October-November 2019) and one at the end (November-December 2020) of our field study, constraining the temperature below 20 °C and RH above 55%, while the reference concentration for the selected data during this period was bracketed within ±10% from the median annual reference concentration (i.e., 467.7 ppb for CO and 19.4 ppb for NO_2). By comparing the resulting Alphasense LCSs median raw signals (i.e., $V_{WEu} - V_{AEu}$) at the beginning and at the end of the measurement period (cf. Fig. 11), a total drift of 86.1 mV is observed for CO and 17.2 mV for NO_2, after one year of operation, corresponding to drifts that are respectively 53 and 68% from the initial signal of the sensors. These values significantly exceed the sensor drifts provided in the specifications of the LCSs, indicating that they increase with a rate that is more than double to that suggested by the manufacturer. This discrepancy can be attributed to the high temperatures and low RHs encountered during our field evaluation, which in some cases exceeded the operational limits set by the manufacturer.

3.5. Compliance with EC guideline standards and data quality objectives

As already reported in the literature, data from LCSs do not meet the quality objectives for use in regulatory observations stated for instance by the associate EC directive as they are not yet adequately robust, and lack innate quality assurance (Peltier et al., 2020; Directive 2008/50/EC, 2008). A key question, however, is whether they can still be used to provide indicative measurements, which require less accuracy and can complement the regulatory observations by increasing the spatiotemporal resolution of AQ measurements. To address this question, the sensors are required to (Directive 2008/50/EC, 2008): 1. have adequate LoD for measuring concentrations below the target/limit value and even lower than the assessment threshold concentrations set by the EC guidelines, 2. provide measurements that fulfil the required minimum data capture and time coverage for indicative measurements, and 3. provide measurements that are within the minimum REU, which according to

the EC legislation should remain within 25% for the two gases that we further analyse here (i.e., CO and NO_2; cf. Section S.6.
in the supplement for more details).

Both CO and NO_2 sensors have sufficiently low LoDs for measuring concentrations in the order of the EC threshold concentrations and even significantly below that. They can also provide rich datasets, achieving data capture and time coverage that is well above the set standard thresholds. Considering the above, the first two requirements mentioned in the previous paragraph are fulfilled, leaving the last as the main limitation for qualifying these LCSs for indicative measurements.

Figure 12 shows the REU of the measurements provided by the Alphasense (Fig. 12a-b) and Winsen (Fig. 12c-d) CO and NO_2 LCSs as a function of the respective reference concentrations. We should note here that the data were averaged over 8 hours for the CO and over 1 hour for NO_2 concentrations, following the EC standard for the limit values; 8600 ppb over 8 hours for CO and 105 ppb over 1 hour for NO_2 (Directive 2008/50/EC, 2008; cf. supplement Table S4). As shown, the sensors did not comply with the required REU limit, even at the beginning of the measurement period when they were not affected by the summer extreme conditions. We should note here, however, that the EC limit value for CO concentrations is much higher compared to those measured at the AQ monitoring station we used in Nicosia, whereas for NO_2 they approached but never exceeded it. Nevertheless, the REU values for the two CO sensors appear to reach a plateau as the concentration of the target gas increases, which was higher for the period after the summer, and even if they are extrapolated to the limit values they would not reach the required 25% threshold. The same is true for the Winsen but not for the Alphasense NO_2 sensor which appears to reach this threshold at concentrations higher than ca. 70 ppb (cf. Fig. 12b), making it the only sensor that can qualify for indicative measurements according to the EC directive.

4 Conclusions

We have investigated the performance of low-cost electrochemical sensors provided by two manufacturers, namely Alphasense and Winsen, for measuring the concentrations of CO, NO_2, O_3 and SO_2. To do so, we carried out yearlong measurements at a traffic AQ monitoring station in Nicosia, Cyprus, where the LCSs were collocated with reference instruments and exposed to highly variable environmental conditions, with extremely high temperatures (up to ca. 45 °C) and low relative humidity conditions (below ca. 10%) during the summer period.

Among the different LCSs tested, the CO sensors exhibited the best overall performance reporting measurements that had high correlation with, and low deviation from, those reported by reference instruments throughout the entire testing period. The NO_2 gas sensors from both manufacturers also exhibited good performance, having satisfactory correlations and deviations when compared to the respective reference instrument. In contrast, the performance of the O_3 sensors was not satisfactory, while the SO_2 sensors were not possible to be evaluated because the ambient concentrations were below their LoDs.

Our measurements demonstrate that the performance of the CO and NO_2 sensors from both manufactures is affected by exposure to temperatures above ca. 25 °C and RH levels below ca. 55%. This is most probably caused by the evaporation of water from the sensor electrolyte, which in turn affects the currents induced by the interaction of the target gases with the

working electrodes through the cells of the sensors. After prolonged use under extreme conditions (i.e., temperatures above ca. 40 °C and relative humidity conditions below ca. 10%) the sensors exhibited high errors, and in some cases technical malfunctions, making them practically unusable. Although the sensors regained their operability (i.e., being able to provide uninterrupted data) as the conditions became milder, their performance did not fully recover. Exposure of the sensors to these

415   extreme conditions appeared to cause a signal drift of more than 50% over a period of a year, which is more than twice faster compared to that indicated by the manufacturers.

Although the LCSs tested in this work fulfilled two of the three criteria (i.e. adequate LoD, measurements that fulfil the required minimum data capture and time coverage) that qualifies them for indicative measurements according to EC standards, they fail the third criterion of exhibiting REU values below 25%. The only exception to this generalisation was the Alphasense

420   NO_2 sensor which exhibited REUs close to 25% for concentrations above 70 ppb, which are below the hourly limit NO_2 value, making it the only LCS that can be used for indicative measurements according to the EC directive.

Code/Data availability

All raw data can be provided by the corresponding authors upon request.

Author contribution

425   RP drafted the manuscript that was reviewed and edited by SB and GB; MC and NH designed and developed the AQ monitors; RP and MD performed the measurements; MS, ES and CS provided the reference station data; RP analysed the data. The research was conceptualised by SB and GB.

Competing interests

The authors declare that they have no conflict of interest.

430   **Acknowledgements**

1. EMME-CARE: This project has received funding from the European Union's Horizon 2020 research and innovation programme under grant agreement No. 856612 and the Cyprus Government.
2. AQ-SERVE: The Project INTEGRATED/0916/0016 (AQ-SERVE) is co-financed by the European Regional Development Fund and the Republic of Cyprus through the Research and Innovation Foundation.
435   3. ACCEPT: The project "ACCEPT" (Prot. No: LOCALDEV-0008) is co-financed by the Financial Mechanism of Norway (85%) and the Republic of Cyprus (15%) in the framework of the programming period 2014 - 2021.

References

AIRPARIF, Available online at: https://commercialisation.esa.int/wp-content/uploads/2020/11/Air-quality-monitoring-in-the-City-of-Paris_Basthiste.pdf

440   Aleixandre, M. and Gerboles, M.: Review of Small Commercial Sensors for Indicative Monitoring of Ambient Gas, J. Chem. Eng. Trans., 30, 169-174, doi:10.3303/CET1230029, 2012.

Alphasense, 2013. Alphasense Application Note AAN106: Humidity Extremes: Drying Out and Water Absorption. Available at: https://www.alphasense.com/wp-content/uploads/2013/07/AAN_106.pdf.

Alphasense, Alphasense Application Note AAN104: How Electrochemical Gas Sensors Work. Available at:
445   https://www.alphasense.com/wp-content/uploads/2013/07/AAN_104.pdf.

Bauerová, P., Šindelárová, A., Rychlík, Š., Novák, Z., Keder, J.: Low-Cost Air Quality Sensors: One-Year Field Comparative Measurement of Different Gas Sensors and Particle Counters with Reference Monitors at Tušimice Observatory, J. Atm., 11, doi:10.3390/atmos11050492, 2020.

Bílek, J., Bílek, O., Maršolek, P. and Bucek, P.: Ambient Air Quality Measurement with Low-Cost Optical and EC Sensors:
450   An Evaluation of Continuous Year-Long Operation, J. Environ., 8(11), 114, doi:10.3390/environments8110114, 2021.

Borrego, C., Costa, A. M., Ginja, J., Amorim, M., Coutinho, M., Karatzas, K., Sioumis, Th, et al.: Assessment of air quality microsensors versus reference methods: the EuNetAir joint exercise, J. Atmos. Environ., 147 (2), 246–263, doi:10.1016/j.atmosenv.2016.09.050, 2016.

Collier-Oxandale, A., Feenstra, B., Papapostolou, V., Zhang, H., Kuang, M., Der Boghossian, B., Polidori, A.: Field and
455   laboratory performance evaluations of 28 gas-phase air quality sensors by the AQ-SPEC program, J. Atmos. Env., 220, doi:10.1016/j.atmosenv.2019.117092, 2020.

Cross, E. S., Williams, L. R., Lewis, D. K., Magoon, G. R., Onasch, T. B., Kaminsky, M. L., Worsnop, D. R., and Jayne, J. T.: Use of EC sensors for measurement of air pollution: correcting interference response and validating measurements, J. Atmos. Meas. Tech., 10 (9), 3575–3588, doi:10.5194/amt-10-3575-2017, 2017.

460   DIRECTIVE 2008/50/EC OF THE EUROPEAN PARLIAMENT AND OF THE COUNCIL, 2008. Official Journal of the European Union, Available online at: https://eur-lex.europa.eu/legal-content/EN/TXT/HTML/?uri=CELEX:32008L0050&from=en

DLI Annual Technical Report Air Quality 2020, Available online at: https://www.airquality.dli.mlsi.gov.cy//sites/default/files/2021-
465   12/Annual%20Air%20Quality%20Technical%20Report%202020_0.pdf

Duvall, R.M., Hagler, G.S.W., Clements, A.L., Benedict , K., Barkjohn, K., Kilaru, V., Hanley, T., Watkins, N., Kaufman, A., Kamal, A., Reece, S., Fransioli, P., Gerboles, M., Gillerman, G., Habre, R., Hannigan, M., Ning, Z., Papapostolou, V., Pope, R., Quintana, P.J.E., Lam Snyder, J.: Deliberating Performance Targets: Follow-on workshop discussing PM10, NO2, CO, and SO2 air sensor targets, Atmos. Environ., 246, 118099, 10.1016/j.atmosenv.2020.118099, 2021.

470 Hagan, D. H., Isaacman-VanWertz, G., Franklin, J. P., Wallace, L. M. M., Kocar, B. D., Heald, C. L. and Kroll, J. H.: Calibration and assessment of EC air quality sensors by co-location with regulatory-grade instruments, J. Atmos. Meas. Tech., 11, 315–328, doi:10.5194/amt-11-315-2018, 2018.

https://www.london.gov.uk/sites/default/files/air_quality_monitoring_guidance_january_2018.pdf

Jerrett, M., Donaire-Gonzalez, D., Popoola, O., Jones, R., Cohen, R. C., Almanza, E., de Nazelle, A., Mead, I., Carrasco-
475 Turigas, G., Cole-Hunter, T., Triguero-Mas, M., Seto, E., Nieuwenhuijsen, M.: Validating novel air pollution sensors to improve exposure estimates for epidemiological analyses and citizen science, J. Environ. Res., 158, 286-294, doi:10.1016/j.envres.2017.04.023, 2017.

Jiao, W., Hagler, G., Williams, R., Sharpe, R., Brown, R., Garver, D., Judge, R., Caudill, M., Rickard, J., Davis, M., Weinstock, L., Zimmer-Dauphinee, S., Buckley, K.: Community Air Sensor Network (CAIRSENSE) project: evaluation of low-cost
480 sensor performance in a suburban environment in the southeastern United States, J. Atmos. Meas. Tech., 9, 5281-5292, doi:10.5194/amt-9-5281-2016, 2016.

Juginovic, A., Vukovic, M., Aranza, I., Bilos, V.: Health impacts of air pollution exposure from 1990 to 2019 in 43 European countries, J. Sci. Rep., 11, doi:10.1038/s41598-021-01802-5, 2021.

Karagulian, F., Barbiere, M., Kotsev, A., Spinelle, L., Gerboles, M., Lagler, F., Redon, N., Crunaire, S., Borowiak, A.: Review
485 of the Performance of Low-Cost Sensors for Air Quality Monitoring, J. Atmosphere, 10, doi:10.3390/atmos10090506, 2019.

Lelieveld, J., Berresheim, H., Borrmann, S., Crutzen, P. J., Dentener, F. J., Fischer, H., Feichter, J., Flatau, P. J., Heland, J., Holzinger, R., Korrmann, R., Lawrence, M. G., Levin, Z., Markowicz, K. M., Mihalopoulos, N., Minikin, A., Ramanathan, V., De Reus, M., Roelofs, G. J., Scheeren, H. A., Sciare, J., Schlager, H., Schultz, M., Siegmund, P., Steil, B., Stephanou, E. G., Stier, P., Traub, M., Warneke, C., Williams, J., and Ziereis, H.: Global air pollution crossroads over the Mediterranean, J.
490 Science, 298, 794–799, doi:10.1126/science.1075457, 2002.

Lelieveld, J., Pozzer, A., Pöschl, U., Fnais, M., Haines, A., Münzel, T.: Loss of life expectancy from air pollution compared to other risk factors: a worldwide perspective, J. Cardiovasc. Res., 116, 1910–1917, doi:10.1093/cvr/cvaa025, 2020.

Lewis, A. C., Lee, J. D., Edwards, P. M., Shaw, M. D., Evans, M. J., Moller, S. J., Smith, K. R., Buckley, J. W., Ellis, M., Gillot, S. R., and White, A.: Evaluating the performance of low cost chemical sensors for air pollution research, J. Faraday
495 Discuss., 189, 85-103, doi:10.1039/c5fd00201j, 2015.

Li, J., Hauryliuk, A., Malings, C., Eilenberg, S.R., Subramanian, R., Presto, A.A.: Characterizing the Aging of Alphasense NO2 Sensors in Long-Term Field Deployments, ACS Sens., 6, 2952-2959, doi:10.1021/acssensors.1c00729, 2021.

Liang, Y., Wu, C., Jiang, S., Li, Y.J., Wu, D., Li, M., Cheng, P., Yang, W., Cheng, C., Li, L., Deng, T., Sun, J.Y., He, G., Liu, B., Yao, T., Wu, M., Zhou, Z.: Field comparison of EC gas sensor data correction algorithms for ambient air measurements,
500 J. Sens. Actuators B Chem., 327, doi:10.1016/j.snb.2020.128897, 2021.

Masson, N., Piedrahita, R. and Hannigan, M.: Quantification Method for Electrolytic Sensors in Long-Term Monitoring of Ambient Air Quality, J. Sens., 15, 27283-27302, doi:10.3390/s151027283, 2015.

Masson, N., Piedrahita, R., and Hannigan, M.: Approach for quantification of metal oxide type semiconductor gas sensors used for ambient air quality monitoring, J. Sens. Actuators B Chem., 208, 339–345, doi:10.1016/j.snb.2014.11.032, 2015.

505 Mead et al., 2013; Smith et al., 2017; Popoola et al., 2016; Hagan et al., 2018, N., Dauge, F. R., Schneider, P., Vogt, M., Lerner, U., Fishbain, B., Broday, D., Bartonova, A.: Can commercial low-cost sensor platforms contribute to air quality monitoring and exposure estimates?, J. Environ. Int., 99, 293-302, doi:10.1016/j.envint.2016.12.007, 2017.

Mead, M.I., Popoola, O.A.M., Stewart, G.B., Landshoff, P., Calleja, M., Hayes, M., Baldovi, J.J., McLeod, M.W., Hodgson, T.F., Dicks, J., Lewis, A., Cohen, J., Baron, R., Saffell, J.R., Jones, R.L.: The use of EC sensors for monitoring urban air

510 quality in low-cost, high-density networks, J. Atmos. Environ., 70, 186-203, doi:10.1016/j.atmosenv.2012.11.060, 2013.

Pang, X., Shaw, M.D., Lewis, A.C., Carpenter, Lucy J., Batchellier, T.: EC ozone sensors: A miniaturised alternative for ozone measurements in laboratory experiments and air-quality monitoring, J. Sens. Actuators B Chem., 240, 829-837, doi:10.1016/j.snb.2016.09.020, 2017.

Peltier, R., Castell, N., Clements, A., Dye, T., Hüglin, C., Kroll, J., Lung, Shih-Chun C., Ning, Z. Parsons, M., Penza, M.,

515 Reisen, F., Schneidemesser, E.: An update on low-cost sensors for the measurement of atmospheric composition, Chairperson, Publications Board World Meteorological Organization (WMO), Geneva 2, Switzerland, 2020.

Popoola, O. A. M., Stewart, G. B., Mead, M. I., Jones, R. L.: Development of a baseline-temperature correction methodology for EC sensors and its implications for long-term stability, J. Atmos. Environ., 147, 330-343, doi:10.1016/j.atmosenv.2016.10.024, 2016.

520 Smith, K. R., Edwards, P. M., Evans, M. J., Lee, J. D., Shaw, M. D., Squires, F., Wilde, S., and Lewis, A. C.: Clustering approaches to improve the performance of low cost air pollution sensors, J. Faraday Discuss., 200, 621-637, doi:10.1039/c7fd00020k, 2017.

Spinelle, L., Gerboles, M., Villani, M.G., Aleixandre, M., Bonavitacola, F.: Field calibration of a cluster of low-cost available sensors for air quality monitoring. Part A: ozone and nitrogen dioxide, J. Sens. Actuators B Chem., 215, 249-257,

525 doi:10.1016/j.snb.2015.03.031, 2015.

Spinelle, L., Gerboles, M., Villani, M.G., Aleixandre, M., Bonavitacola, F.: Field calibration of a cluster of low-cost commercially available sensors for air quality monitoring. Part B: NO, CO and CO2, J. Sens. Actuators B Chem., 238, 706-715, doi:10.1016/j.snb.2016.07.036, 2017.

Vrekoussis, M., Pikridas, M., Rousogenous, C., Christodoulou, A., Desservettaz, M., Sciare, J., Richter, A., Bougoudis, I.,

530 Savvides, C., Papadopoulos, C. Local and regional air pollution characteristics in Cyprus: A long-term trace gases observations analysis, J. Sci. Total Environ., 845, 157315, doi:10.1016/j.scitotenv.2022.157315, 2022.

Walker, S. E., Schneider, P. A study of the relative expanded uncertainty formula for comparing low-cost sensor and reference measurements, NILU, ISBN: 978-82-425-2997-8, 2020.

World Meteorological Organization (WMO), Low-cost sensors for the measurement of atmospheric composition: overview of

535 topic and future applications. Lewis, A. C., von Schneidemesser, E. and Peltier R. E. (Eds), Geneva, Switzerland, 2018.

Zimmerman, N., Presto, A.A., Kumar, S.P.N., Gu, J., Hauryliuk, A., Robinson, E.S., Robinson, A.L., Subramanian, R.: A machine learning calibration model using random forests to improve sensor performance for lower-cost air quality monitoring, J. Atmos. Meas. Tech., 11, 291-313, doi:10.5194/amt-11-291-2018, 2018.

Figure 1: Images showing the layout of the AQ monitors housing the Alphasense (a) and the Winsen (b) LCSs, the side of the AQ monitors at which the sensing elements of the LCSs were exposed to the ambient air (c), and the place that the AQ monitors were installed at the top of the reference station (d).
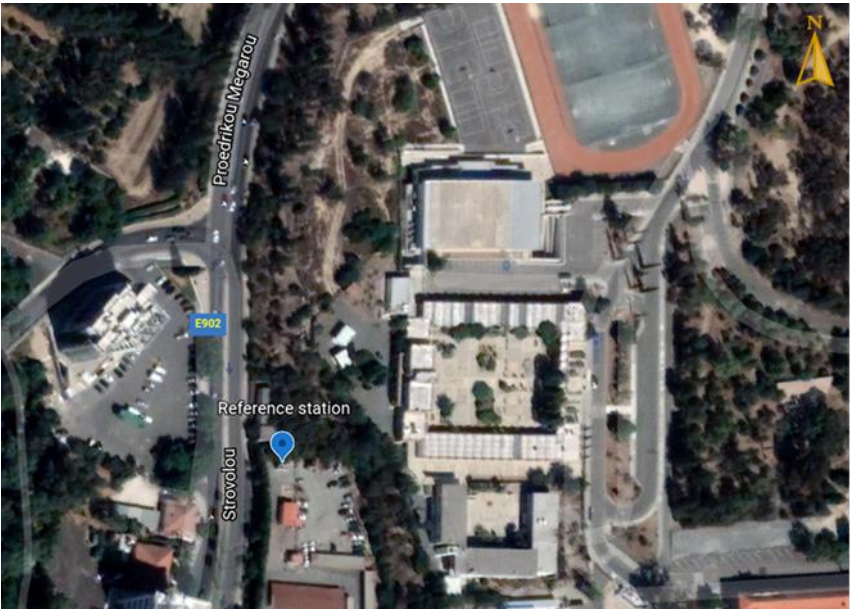
Figure 2: Satellite image showing the location of the traffic AQ monitoring station in Nicosia where the measurements were carried out. The station is located ca. 10 m from Strovolou avenue, which is a rather busy road especially during the morning and afternoon rush hours. Map data are from © Google, DigitalGlobe.
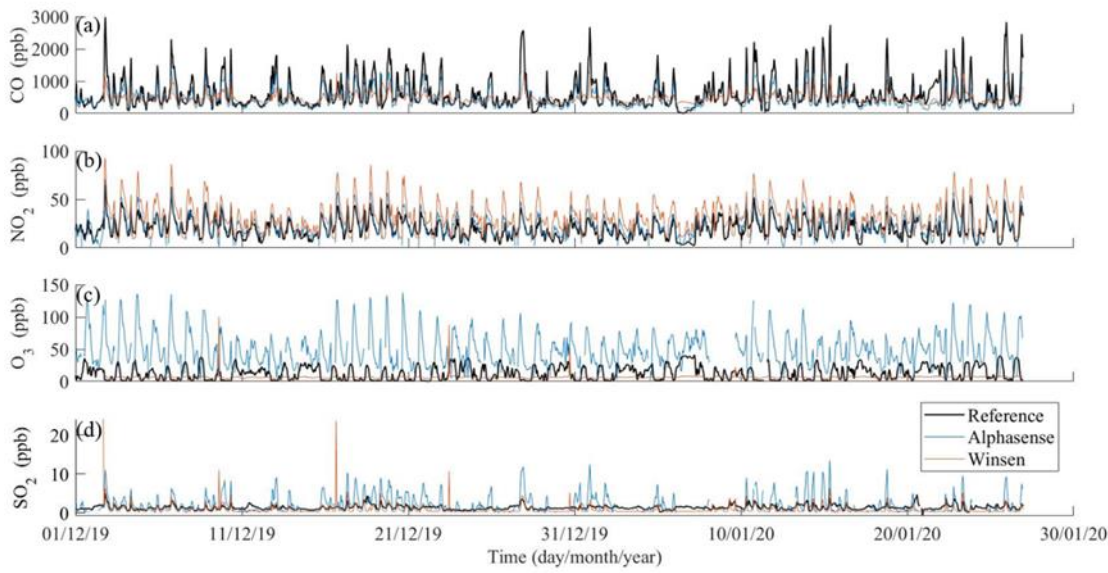
Figure 3: Time series of hourly averaged concentrations measured by the Alphasense and Winsen EC gas sensors and the reference instruments from 1 December 2019 to 26 January 2020 for CO (a), NO₂, (b), O₃ (c) and SO₂ (d). We should note here that the data from the LCSs were determined through the calibration equations discussed in Section 2.4 (for the Alphasense sensors) or provided directly by the sensors (for the Winsen sensors). Exception to this are the data from the Winsen CO LCS, for which we subtracted 400 ppb from all the measurements, and the SO₂ LCSs from both manufacturers were the signal was divided by a factor of 10 for illustration purposes.

Table 1: Summary statistics, including the number of hourly averaged data points used for data analysis of each LCS (N), and the mean concentration of hourly averaged gaseous concentrations measured by the Alphasense and Winsen LCSs and the reference instruments for the entire study period, together with the Standard Deviation (SD) for each case, as well the associated values of the MRE, MBE, MAE and R^2. The LoD values for each LCS are also provided for comparison. In addition, the slope and intercept of the linear regression for each sensor are given as per U.S EPA (Duvall et al., 2021).

Type of sensor	LCS N	LCS Mean ± SD	Reference Mean ± SD	MRE (%)	MBE (ppb)	MAE (ppb)	LoD (ppb)	Linear regression parameters		
								Slope	Intercept	R^2
Alphasense CO	5798	427.8 ± 268.8	646.0 ± 595.4	-4.7	-218.2	288.8	4	1.60	-52.7	0.54
Winsen CO[1]	3784	419.6 ± 156.3	531.1 ± 412.0	35.1	-111.3	256.3	130	1.30	-23.2	0.25
Alphasense NO₂	4126	22.9 ± 13.1	22.6 ± 18.1	53.7	0.29	10.8	15	0.44	12.5	0.10
Winsen NO₂	3900	31.3 ± 19.3	19.6 ± 12.5	104.8	11.7	15.1	15	0.34	8.7	0.29
Alphasense O₃	4728	74.6 ± 55.8	27.5 ± 23.8	923.1	41.5	48.1	15	0.10	18.8	0.05
Winsen O₃	3879	10.2 ± 23.4	20.8 ± 18.3	44.0	-10.6	16.5	15	0.20	18.8	0.06
Alphasense SO₂	3864	23.3 ± 22.8	1.8 ± 1.0	1354.4	21.5	21.6	5	0.02	1.4	0.12
Winsen SO₂	3888	7.1 ± 7.6	1.5 ± 0.65	389.5	5.6	5.6	15	0.04	1.3	0.17

---

[1] Measurements recorded by the Winsen CO sensors were reduced by 400 ppb in order to better match the measurements from the reference instruments. The Winsen CO statistics provided in this Table correspond to the corrected data.
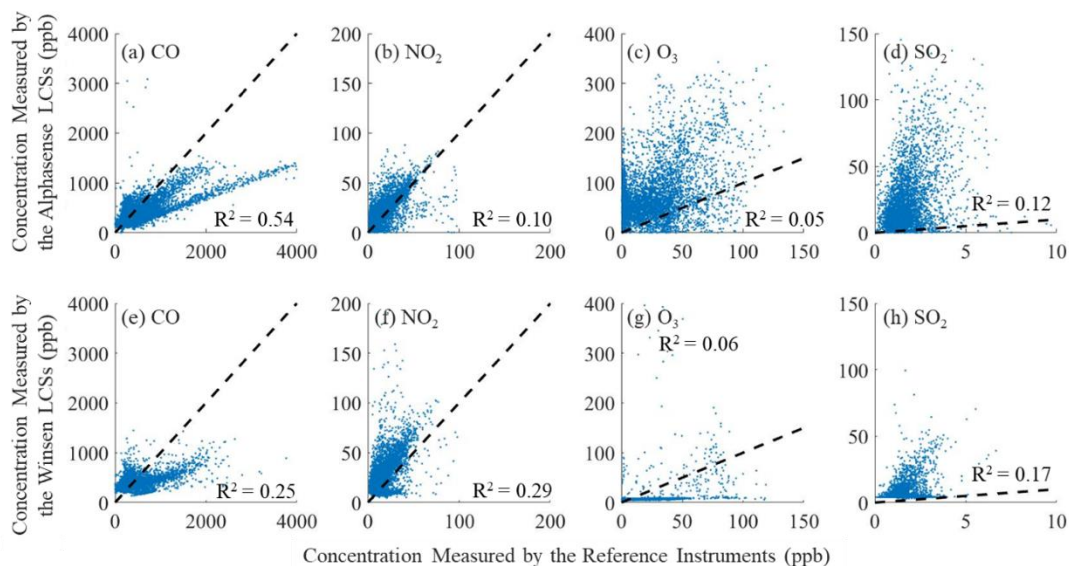
Figure 4: Correlation between the measurements recorded by the Alphasense (a-d) and Winsen (e-h) LCSs and those provided by the respective reference instruments. The black dashed lines indicate the 1:1 line. Measurements from the O_3 and SO_2 LCSs by both manufacturers do not have the same x-y axis scales due to the big difference between reference and LCSs measurements recorded.
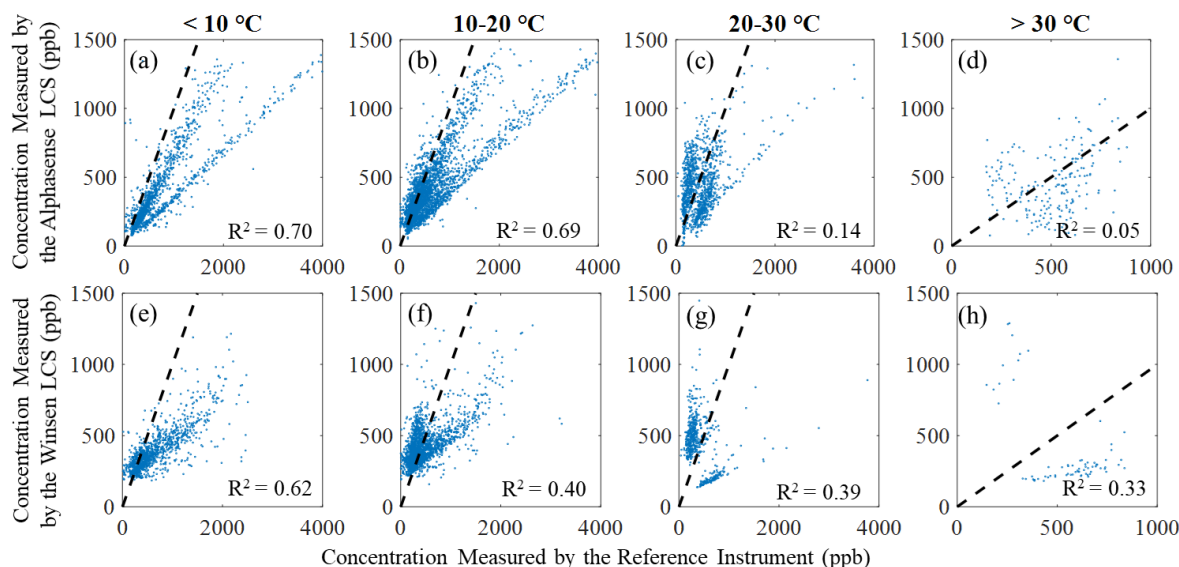
Figure 5: Correlation between the CO measurements recorded by the Alphasense (a-d) and the Winsen (e-h) LCSs, and those provided by the respective reference instrument at four different temperature ranges. The 1:1 lines in each subplot are depicted as dashed lines.
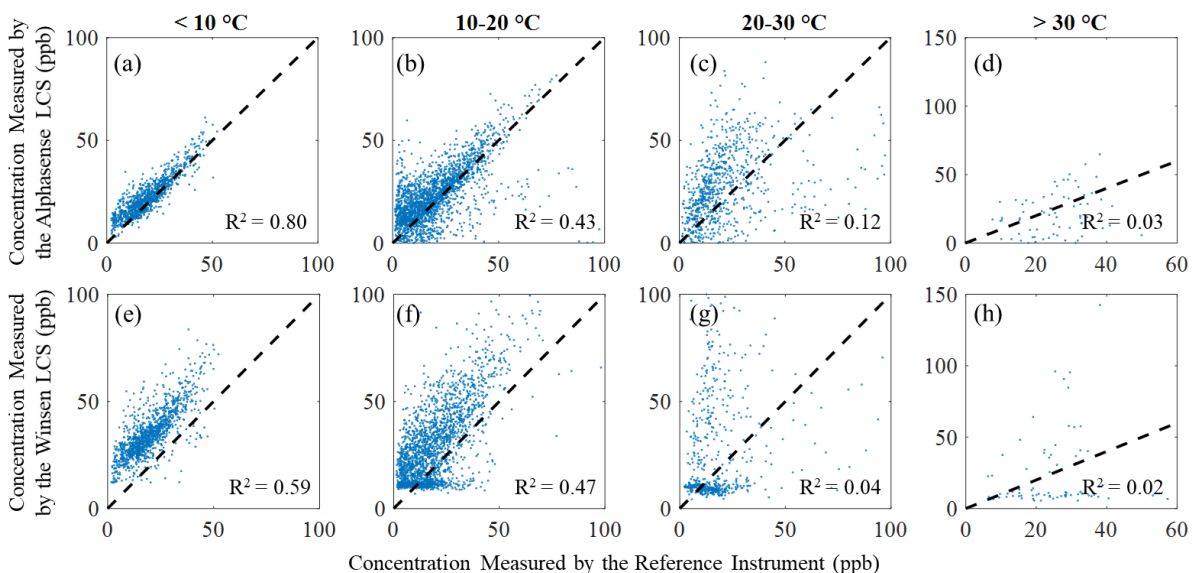
Figure 6: Correlation between the NO₂ measurements recorded by the Alphasense (a-d) and the Winsen (e-h) LCSs and those provided by the respective reference instrument at four different temperature ranges. The 1:1 lines in each subplot are depicted as dashed lines.

Table 2: Summary statistics including the number of hourly averaged data points (N) and the MRE for each LCS at four different temperature ranges over the entire study period. Linear regression parameters including NRMSE, slope, intercept and R^2 are also provided for each temperature range.

Type of sensor	Temperature range (°C)	N	MRE (%)	Linear regression			
				NRMSE	Slope	Intercept (ppb)	R^2
Alphasense CO	< 10	1287	-28.5	0.38	0.36	139.2	0.70
	10-20	3138	-4.1	0.35	0.34	193.0	0.69
	20-30	1170	17.2	0.50	0.24	318.5	0.14
	>30	203	9.4	0.66	0.41	278.3	0.05
Winsen CO	< 10	1149	-9.5	0.23	0.25	227.1	0.62
	10-20	2008	55.5	0.26	0.24	309.1	0.40
	20-30	547	54.7	0.38	-0.10	494.1	0.39
	> 30	71	7.7	0.63	-0.95	907.7	0.33
Alphasense NO₂	< 10	1087	30.3	0.38	0.34	14.9	0.80
	10-20	2232	62.7	0.58	0.19	17.6	0.43
	20-30	765	65.7	0.56	0.29	20.18	0.12
	> 30	42	-35.1	0.76	0.10	12.5	0.03
Winsen NO₂	< 10	1175	111.6	0.21	0.87	17.6	0.59
	10-20	2089	103.4	0.45	0.97	10.8	0.47
	20-30	556	109.4	1.00	0.44	22.0	0.04
	> 30	71	8.7	1.11	0.40	14.2	0.02
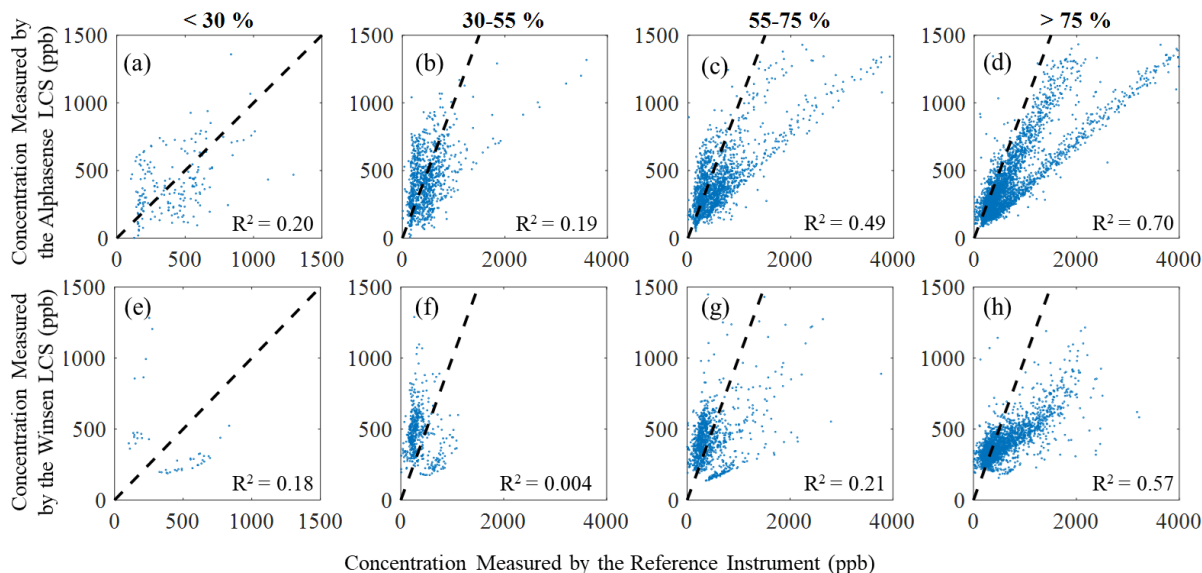
Figure 7: Correlation between CO measurements recorded by the Alphasense (a-d) and the Winsen (e-h) LCSs and those provided by the respective reference instrument at four different RH ranges. The 1:1 lines in each subplot are depicted as dashed lines.

600
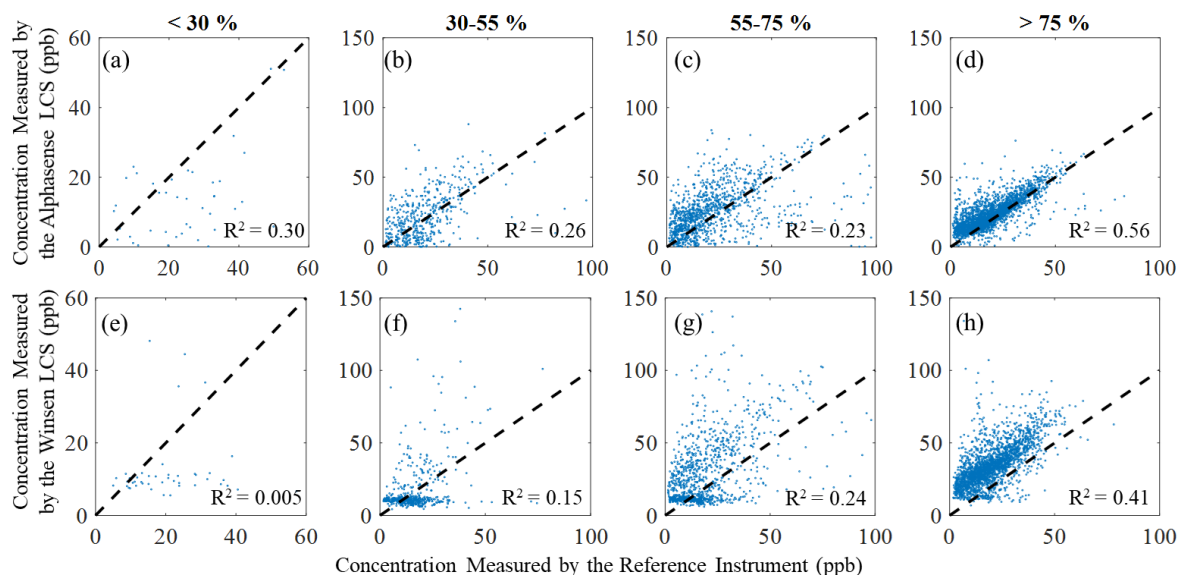
Figure 8: Correlation between the NO_2 measurements recorded by the Alphasense (a-d) and the Winsen (e-h) LCSs and those provided by the respective reference instrument at four different RH ranges. The 1:1 lines in each subplot are depicted as dashed lines.

Table 3: Summary statistics including the number of hourly averaged data points (N) and the MRE for each LCS at four different RH ranges over the entire study period. Linear regression parameters including NRMSE, slope, intercept and R² are also provided for each RH range.

Type of sensor	RH range (%)	N	MRE (%)	Linear regression fitting			
				NRMSE	Slope	Intercept (ppb)	R^2
Alphasense CO	< 30	189	18.9	0.48	0.44	219.6	0.20
	30-55	1011	21.3	0.49	0.30	289.4	0.19
	55-75	1631	4.3	0.44	0.32	220.4	0.49
	> 75	2967	-20.1	0.37	0.35	171.3	0.70
Winsen CO	< 30	44	56.1	0.19	-0.50	603.1	0.18
	30-55	500	92.6	0.26	-0.09	497.8	0.004
	55-75	1005	67.0	0.36	0.18	343.0	0.21
	> 75	2229	6.7	0.29	0.24	261.0	0.57
Alphasense NO₂	< 30	25	-25.8	0.88	0.31	5.9	0.30
	30-55	459	37.7	0.64	0.36	12.2	0.26
	55-75	1182	62.7	0.65	0.15	20.2	0.23
	> 75	2460	53.2	0.44	0.27	17.1	0.56
Winsen NO₂	< 30	44	-26.4	0.78	0.06	11.1	0.005
	30-55	521	41.3	0.99	0.73	6.02	0.15
	55-75	1037	115.3	0.70	0.80	14.9	0.24
	> 75	2292	117.3	0.32	0.84	17.9	0.41
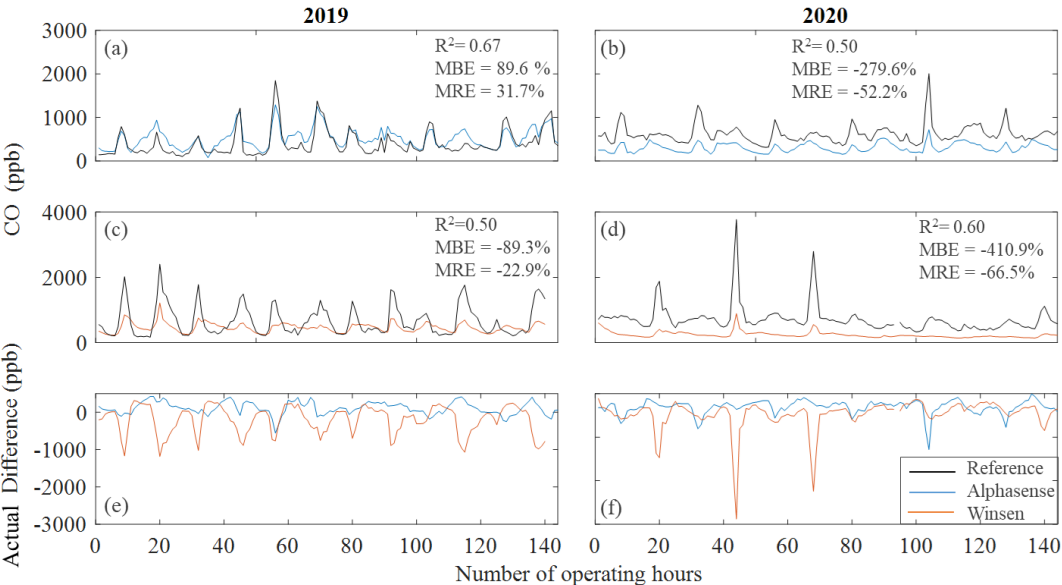
Figure 9: Time series of hourly-averaged concentrations measured by the Alphasense (a-b) and Winsen (c-d) CO LCSs over six-consecutive days at the beginning (left column; October 2019 for Alphasense and November 2019 for Winsen) and at the end (right column; October 2020 for Alphasense and September 2020 for Winsen) of our measurement period. Last row shows the concentration actual difference between CO LCSs and reference instrument in 2019 (e) and 2020 (f).
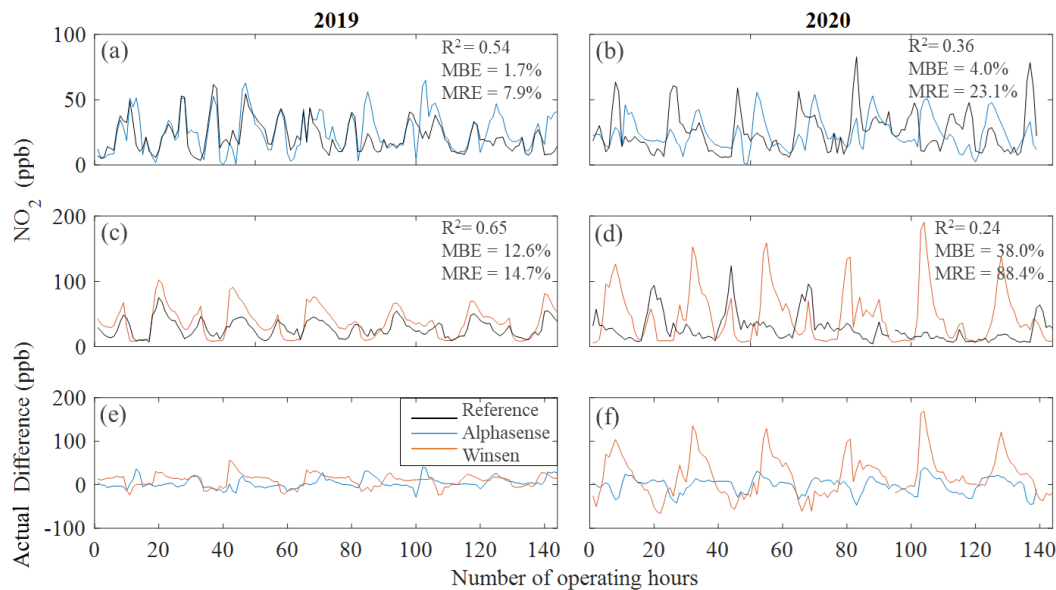
Figure 10: Time series of hourly-averaged concentrations measured by the Alphasense (a-b) and Winsen (c-d) NO₂ LCSs over six-consecutive days at the beginning (left column; October 2019 for Alphasense and November 2019 for Winsen) and at the end (right column; October 2020 for Alphasense and September 2020 for Winsen) of our measurement period. Last row shows the concentration actual difference between CO LCSs and reference instrument in 2019 (e) and 2020 (f).

Table 4: Median values of CO and NO₂ LCSs NMREs over 6 consecutive days at the beginning (2019) and at the end (2020) of the measurement period, and the respective median values of temperature, RH and reference concentrations.

	NMRE	Median Temperature (°C)		Median RH (%)		Median Reference Concentration (ppb)	
		2019	2020	2019	2020	2019	2020
Alphasense CO	-2.6	22.3	21.6	56.2	66.8	298.0	576.7
Alphasense NO₂	1.9	21.0	20.5	64	70.1	18.4	22.4
Winsen CO	2.0	12.8	26.3	74.8	61.4	458.9	649.5
Winsen NO₂	1.3	12.8	26.3	75.0	61.65	25.6	22.2
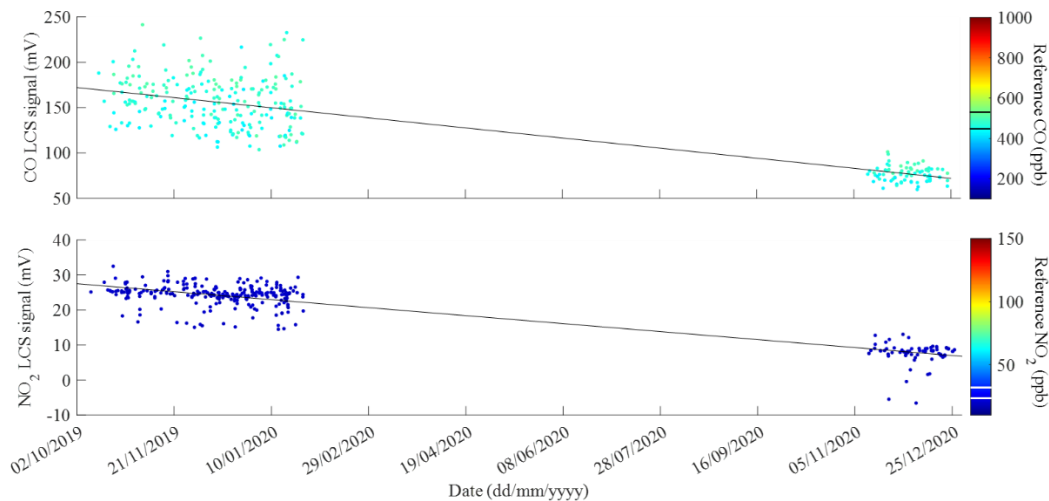
Figure 11: Signal drift of the (a) CO and (b) NO₂ Alphasense LCSs over a period of a year. The data were selected such that the reference concentration is within ±10% from the median annual reference concentration (i.e., 467.7 ppb for CO and 19.4 ppb for NO₂, cf. solid lines on colour bars), whereas the temperature and RH where constrained below 20 °C and above 55%, respectively.
The solid line shows linear fitting through these measurements.
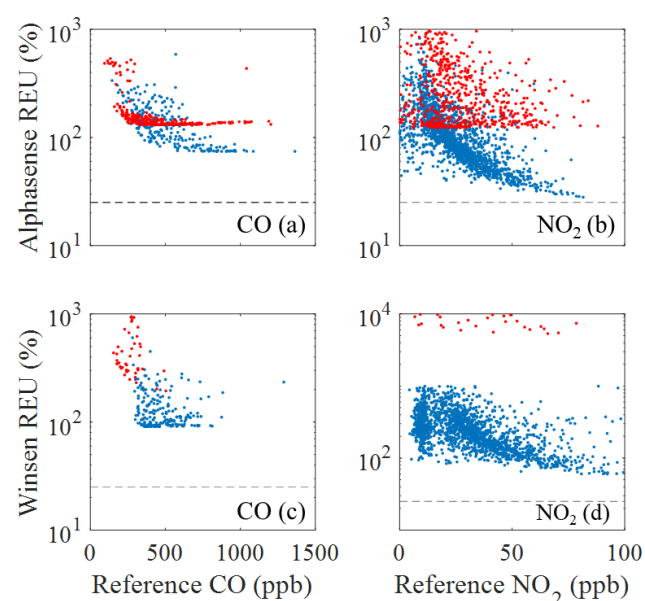
Figure 12: Relative expanded uncertainty of the 8-hour averaged CO (a and c) and the hourly averaged NO₂ (b and d) measurements of the LCSs tested in this study. The values shown here were determined using the methodology described on the AQ Directive 2008/50/EC. The limit values suggested by the EC directive are indicated by the horizontal dashed black line. Data shown are divided into two time periods: before (blue dots) and after (red dots) summer 2020.